Observation of Three Behaviors in Confined Liquid Water within a Nanopool Hosting Proton-Transfer Reactions

ARTICLE *in* THE JOURNAL OF PHYSICAL CHEMISTRY B · JUNE 2007

Impact Factor: 3.3 · DOI: 10.1021/jp068764+ · Source: PubMed

Observation of Three Behaviors in Confined Liquid Water within a Nanopool Hosting Proton-Transfer Reactions

Abderrazzak Douhal,* Gonzalo Angulo, Michal Gil, Juan Ángel Organero, Mikel Sanz, and Laura Tormo

Departamento de Química Física, Sección de Químicas, Facultad de Ciencias del Medio Ambiente, Universidad de Castilla-La Mancha, Avenida Carlos III, S.N., 45071 Toledo, Spain

Received: December 20, 2006; In Final Form: March 1, 2007

In this contribution, we report on studies of rotational and diffusional dynamics of 7-hydroxyquinoline (7HQ) within a reverse micelle (RM) containing different amounts of water. Analyzed in terms of the wobbling-in-a-cone model, the data reveal structural and dynamical properties of the nanopool. We clearly observed three regions in the behavior of confined water molecules within the RM hosting a double proton-transfer reaction between the probe and water. This observation remarkably reproduces the change of calculated water density within this life-mimicking medium. The number of water molecules per AOT head in the transition regions changes from 2 to 5, the latter being very near to the full solvation number (6) of the RM heads. Moreover, the H-bonds breaking and making within the RM to give new structures of the probe strongly affect the environment fluidization in different extents, reflected in different relaxation times of these structures; however, they are of similar sizes. We discuss the role of RM confinement and the proton-transfer dynamics on the behavior of water and their relationships to the packing of water molecules in the studied range of concentrations.

1. Introduction

Water is everywhere, and it is the signature of life. However, it does not behave in biological media as it does in bulk.[1,2] Attempts to characterize precisely its properties in the vicinity around protein pockets and cell membranes have been done, but the complexity of the used systems stimulates searches for simpler ones mimicking biological media.[2] Reverse micelles (RM) constitute a good and extensively used alternative, and that formed by sodium bis(2-ethylhexyl) sulfosuccinate (AOT) in apolar solvents is one of the most studied media (Scheme 1).[3−5] Many groups have reported on the behavior of dyes embedded in the water nanopools of different water content (defined by the ratio of total water to surfactant concentrations, $W_0 = [H_2O]/[AOT]$) therein formed.[6−13] The use of fluorescent dyes with functional groups able to accept or donate hydrogen atoms or protons to water in the nanopool is a quite logical choice because of this ubiquitous reaction in living systems.[14]

Therefore, several reports on the ultrafast behavior of water enclosed in RM have revealed very interesting features.[15−18] For example, time-resolved infrared pump−probe experiments have shown a biexponential orientational relaxation of the excited OD stretching mode below $W_0 = 10$, and a strong retardation at low water concentrations.[15a] Terahertz experiments have also shown a biexponential behavior of the dielectric relaxation of water in the nanopool and suppression of the fast component at low W_0 because of the confinement.[16] Vibrational energy transfer between water molecules becomes slower than that in bulk water, and it is strongly linked to the confinement of water in the nanopool and the weakening of the H-bonding.[17] These confinement effects are also well-known in photoionization studies, in which both kinetics of attachment of isooctane solvated electrons to the water nanopools and the solvated electron absorption spectrum show a RM size dependency.[18]

Recently,[19] we reported on the fluorescence of 7-hydroxyquinoline (7HQ) in AOT RM (Scheme 1). Previous studies of 7HQ have reported on its spectral and dynamical behaviors in several media (gas, liquid, and matrices).[20] Now, we extend our recent work by presenting a time-resolved fluorescence anisotropy study. We have measured the picosecond (ps) anisotropy decays of 7HQ prototropic species at different water concentrations in the AOT microemulsions. The results show different behaviors of the interrogated structures of the probe, and the data have been analyzed by means of the wobbling-in-a-cone (WIC) model.[21] This simple model has the advantage of providing straightforwardly an order parameter related to the movement restriction of the probe molecule, as well as two relaxation times related to the wobbling motion of the probe and its lateral diffusion. The water content effect on these parameters gives insight into the environment structure and ps-dependencies surrounding the probe.[12,22,23] The result shows how the water nanopool is interrogated by the proton-transfer reactions experienced by the probe. A remarkable coincidence between the changes of the relaxation times of the different structures of the probe and of the density of micellar water when changing the number of water molecules within the micelle provides the clues to help us understand why and at which water content the confinement of the micelle affects the observed dynamics.

2. Materials and Methods

7-hydroxyquinoline (7HQ) (Acros, 99%), *n*-heptane (Acros, Spectrograde), and sodium bis(2-ethylhexyl) sulfosuccinate (AOT) (Fluka, Ultra >99%) were used as received. The Karl Fischer test shows that the percentage of water in the *n*-heptane

* Corresponding author. E-mail: Abderrazzak.douhal@uclm.es. Fax: + 34-925-268840.

10.1021/jp068764+ CCC: $37.00
Published on Web 04/24/2007

SCHEME 1: (A) Structures of Enol and Keto-type Forms of 7HQ, Water, and AOT; (B) Representation of 7HQ/H_2O into AOT/*n*-heptane RM[a]

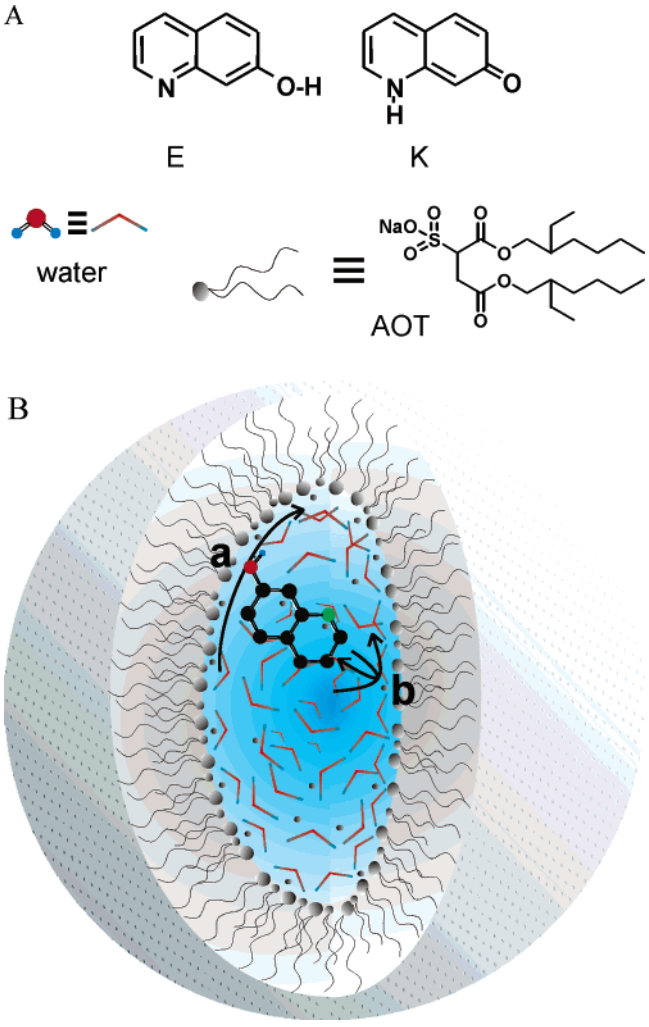

[a] The arrows illustrate (a) the lateral diffusion motion and (b) the wobbling of the probe within the RM.

RM solution is about 0.15% w/v. So without adding water the RM already has a $W_0 \approx 0.6$. Milli-Q ultrapure water was used in all experiments. To test the change of the water network in the nanopool, its relative concentration ($W_0 = [H_2O]/[AOT]$) was increased by adding appropriate amounts to a stock solution. The used 7HQ concentration was low enough (5×10^{-4} M) to guarantee less than one probe molecule per RM, and the AOT concentration in *n*-heptane (0.2 M) was in the range of monodispersivity for all W_0 studied.[24] Picosecond (ps) time-resolved emission measurements were done by using a time-correlated single-photon counting spectrophotometer (FluoTime 200) exciting at 371 nm (fwhm of the instrument response function (IRF) = 65 ps).[25] The anisotropy decay curves were fitted by multiexponential functions convoluted with the IRF using the Fluofit package. The quality of the fits was characterized in terms of residual distribution, its autocorrelation and the reduced χ^2 value. Then, these functions were used to extract the WIC parameters

$$r(t) = r_0[S^2 + (1 - S^2)\exp(-t/\tau_R)]\exp(-t/\tau_D) \qquad (1)$$

with $S = {}^1/_2 \cos\theta(1 + \cos\theta)$, where r_0 is the anisotropy at $t = 0$, S is the order parameter (equal to zero for completely free motion and one for completely restricted), τ_R is the wobbling relaxation time, τ_D is the lateral diffusion relaxation time, and θ is the cone (revolution cone defined by the wobbling motion) angle.[21] A pictorial representation of the WIC model is shown in Scheme 2. The experiments were done at 293 ± 1 K.

SCHEME 2: Representation of the Wobbling-in-Cone Motion of a Probe[a]

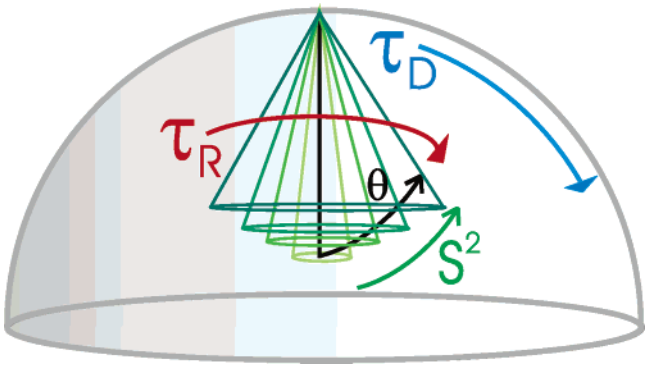

[a] τ_R is the wobbling relaxation time, τ_D is the lateral diffusion relaxation time, S^2 is the square of the order parameter, and θ is the cone semi-angle, increasing with the fluidity of the environment.

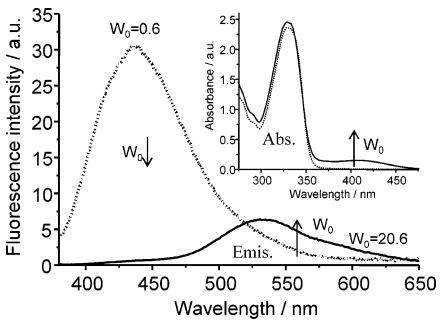

Figure 1. Emission spectra (excitation at 371 nm) and absorption (inset) of 7HQ in AOT/*n*-heptane reverse micelles (RM) for W_0 = 0.6 (dotted) and 20.6.

3. Results and Discussion

Depending on the pH of water, four different prototropic species of 7HQ might be present: enol (E), another tautomer (K) (either zwitterionic or ketonic), and anionic (A) and cationic (C) structures.[20] For the used RM and in the absence of added water, only the E absorption can be observed (Figure 1, inset). The emission shows a band at 430 nm attributed to a strongly bound form of E to the AOT head groups (E···AOT) (Figure 1).[19] The bonded structure should have an anionic character where the O−H proton of E is shared with the AOT head groups. As W_0 increases (from 0.6 to 20.6), a band in the absorption spectrum at 410 nm grows up, while the emission band of the E···AOT form shifts up 10 nm and decreases in intensity. Concomitantly, the K emission centered at 530 nm appears and grows up without any significant shift. The observation of the 410 nm band in absorption in the presence of water indicates the formation of strongly H-bonded complexes between E and the nanopool water molecules, leading to A forms of 7HQ emitting at 505 nm. The emission of K (530 nm) reflects the production of a double proton-transfer reaction in bound E. The fluorescence decays of these structures have been reported and discussed elsewhere.[19] Briefly, a two-step mechanism has been proposed to explain the results: a direct formation of K from bound E via a water-assisted double proton-transfer reaction, and consecutive reactions involving the formation and disappearance of A to give K. The emission

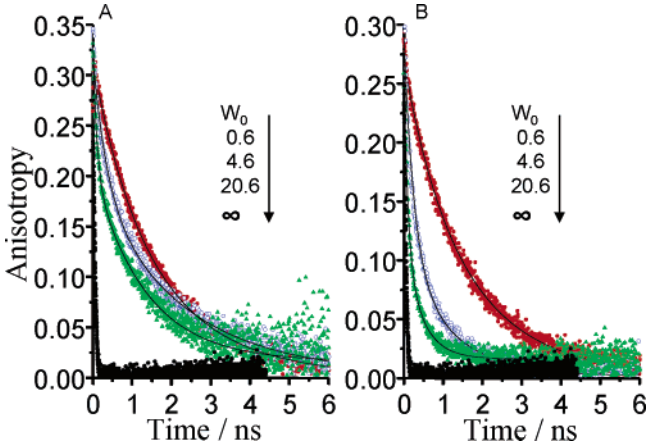

Figure 2. Anisotropy decays of 7HQ in water/AOT/*n*-heptane RM for $W_0 = 0.6$, 4.6, and 20.6 at 450 and 530 nm and in pure water (∞) at 460 and 505 nm. The solid lines are from the best experimental fit. The arrows indicate the evolution of the decays as W_0 increases. Excitation wavelength: 371 nm.

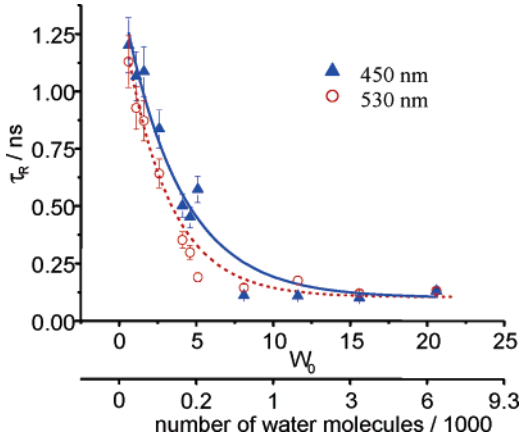

Figure 3. Effect of water content on the wobbling relaxation-time values of 7HQ in water/AOT/*n*-heptane RM at 450 nm (full triangles) and 530 nm (empty circles). The lines are drawn just to guide the eyes. The bottom axis shows the number of water molecules inside the nanopool.

anisotropy experiments presented here interrogate the bound E and A (450 nm) and the K (530 nm) forms. We have studied the system using a wide range of W_0 (from 0.6 to 20.6).

Figure 2 shows four representative anisotropy decays of the emission at 450 and 530 nm, upon 371 nm excitation of 7HQ in pure water and in RM. Biexponential functions reproduce the decays very well. The data are shown in Table 1. The initial anisotropy value (r_0) is quasi-invariant with W_0: close to 0.35 ± 0.05 at 450 nm and to 0.30 ± 0.04 at 530 nm. The difference is because the 450 nm emission band corresponds to that of directly excited bound E, whereas the 530 nm one originates mostly after a double proton-transfer reaction at S_1. The difference in the transition dipole moment angles between both forms can be calculated from $r_0 = \{(3\cos^2\varphi - 1)\}/\{5\}$ where φ is the angle formed by the absorption and emission transition dipole moments, and it results $\Delta\varphi = 7°$. This difference may come from either a different orientation of the emission dipole moments of both forms or from the rotation of 7HQ (E or A) during the formation of K. Note also that at 371 nm the A bound form absorbs giving K.[19]

The anisotropy decays in the absence of added water are relatively slow and are very similar at both detection wavelengths. However, the decays become shorter when the water content of the RM increases (Figure 2). It is noteworthy that the long time (2.12 ns) component at $W_0 = 0.6$ (Table 1) is comparable to the decay time (1.81 ns) of the solvent correlation function ($C(t)$) measured previously in the absence of added water.[19] This similarity suggests a close relationship between the physical processes behind both $r(t)$ and $C(t)$ behaviors of E-AOT in the absence of added water. In the presence of water, the short decay time component (τ_1) shows the same trend for both forms (Table 1). However, above $W_0 = 4$ the longest one (τ_2) of the bound E (450 nm) is twice that of K (530 nm), but it is below this value for both forms (2.12 to 1.34 ns for E bound and 2.12 to 0.46 ns for K, going from $W_0 = 0.6$ to 20.6, see Table 1). For an oblate of the shape and size of 7HQ, the rotational relaxation time in pure water, calculated under stick boundary conditions, is 35 ps. This value is ~3 times shorter than the shortest time measured in these experiments but close to the one (40 ps) recorded in pure water (Table 1).

Little information can be obtained from the former analysis. Therefore, to get parameters relevant to the structural changes within the nanopool, we have analyzed the anisotropy decays by means of the WIC model (eq 1).[21] This model has been used successfully to analyze the anisotropy behavior in polymers, micelles, membranes, and proteins.[26−28] Figures 3−5 show the results of such analysis in the range of W_0 measured. The wobbling relaxation time (τ_R) decreases monotonically from 1.2 to 0.1 ns for both forms (Table 2, Figure 3). However, the lateral relaxation time (τ_D) shows a quite different behavior (Table 2, Figure 4). For both forms, this time reaches a maximum at $W_0 \approx 2$, and a plateau after $W_0 \approx 5$, with a τ_D value about 3 times larger for the bound E (1.34 ns) than for the K one (0.46 ns).

Concurrently, the square of the order parameter (S^2) is larger for bound E in the whole range of W_0 (Table 2, Figure 5), reflecting that the E motion is more restricted than that of K. As W_0 increases, the S^2 value for E decreases from 0.82 to 0.53,

TABLE 1

	λ_{em} = 450 nm (460 nm for pure water, ∞)				λ_{em} = 530 nm (505 nm for pure water, ∞)			
W_0	τ_1/ns	%A_1	τ_2/ns	%A_2	τ_1/ns	%A_1	τ_2/ ns	%A_2
0.6	0.92	37.5	2.12	62.5	0.74	35.7	2.12	64.3
1.1	0.69	17.1	1.99	82.9	0.63	29.6	1.99	70.4
1.6	0.72	25.8	2.24	74.2	0.63	40.7	2.24	59.3
2.6	0.71	41.4	2.82	58.6	0.62	63.6	2.82	36.4
4.1	0.51	48.5	2.70	51.5	0.40	72.0	2.70	28.0
4.6	0.38	35.7	2.25	64.3	0.24	54.2	1.19	45.8
5.1	0.30	29.6	1.87	70.4	0.14	41.7	0.82	58.3
8.1	0.10	44.7	1.28	55.3	0.12	64.5	0.71	35.5
11.6	0.10	48.7	1.26	51.3	0.14	68.2	0.79	31.8
15.6	0.09	52.4	1.18	47.6	0.10	60.0	0.50	40.0
20.6	0.10	42.4	1.34	57.6	0.10	61.5	0.46	38.5
∞	0.04	100			0.04	100		

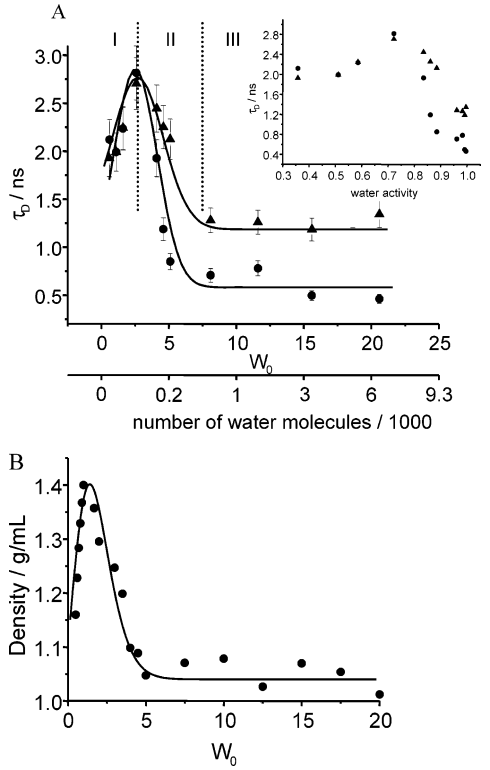

Figure 4. (A) Changes of lateral diffusion relaxation times with W_0 for 7HQ in water/AOT/*n*-heptane RM at 450 nm (full triangles) and 530 nm (full circles). The bottom axis shows the corresponding number of water molecules inside the nanopool. Inset: the same as function of the water activity as taken from ref 3b. (B) Variation of the average density of water inside the AOT/*n*-heptane RM with W_0. Lines are drawn just to guide the eye.

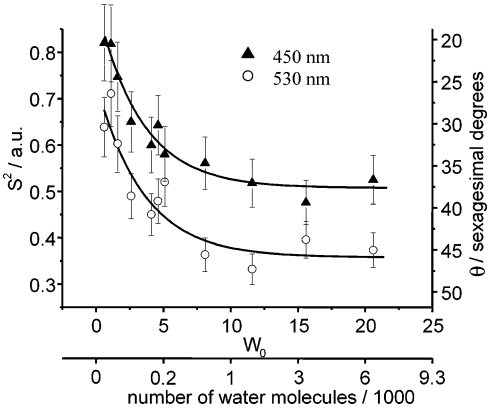

Figure 5. Variation of the square of order parameter (S^2) with W_0 for 7HQ in water/AOT/*n*-heptane RM at 450 nm (full triangles) and 530 nm (empty circles). The right axis shows the equivalent cone semiangles. The lines are drawn just to guide the eyes. The bottom axis gives the number of water molecules inside the nanopool.

while it goes from 0.64 to 0.37 for K. A change in the decrease of motion is comparable for both structures, keeping the difference in freedom almost constant. By using the correspondence between S^2 and the semicone angle θ of the revolution cone defined by the wobbling motion, we found a difference of $8 \pm 2°$ between the values of θ for both forms in the whole studied range of W_0.

Note that for τ_R, τ_D, and $S^2(\theta)$ there is little or no change above $W_0 \approx 5$. Therefore, three W_0 regions for the behavior of confined water in the nanopools can be distinguished from the previous observations, as depicted in Figure 4. Region I in which W_0 goes from 0.6 to 2 and for which τ_D increases from 2 to ~3 ns. Region II corresponds to $W_0 = 2-5$ values and in which τ_D now decreases to 2 ns for bound E and to 1 ns for K. Region III reflects the behavior at $W_0 > 5$, common to all WIC parameters and where no significant changes are observed. Two transitions ($W_0 = 2$ and 5) are then observed in the structural change within the RM

TABLE 2

	$\lambda_{em} = 450$ nm				$\lambda_{em} = 530$ nm			
W_0	τ_R/ns	τ_D/ns	S^2	q	τ_R/ns	τ_D/ns	S^2	q
0.6	1.20	1.93	0.82	21	1.13	2.12	0.64	31
1.1	1.07	1.99	0.82	21	0.93	1.99	0.71	27
1.6	1.09	2.24	0.75	25	0.87	2.24	0.60	33
2.6	0.84	2.71	0.65	30	0.64	2.815	0.49	38
4.1	0.50	2.45	0.60	33	0.35	1.93	0.45	40
4.6	0.45	2.25	0.64	31	0.30	1.19	0.48	39
5.1	0.57	2.13	0.58	34	0.19	0.85	0.52	37
8.1	0.11	1.28	0.56	35	0.15	0.71	0.36	45
11.6	0.11	1.26	0.52	37	0.18	0.78	0.33	47
15.6	0.10	1.18	0.48	39	0.12	0.50	0.40	43
20.6	0.13	1.34	0.53	37	0.13	0.46	0.37	44

One of the widely used models to describe the structure of a RM containing water is the core−shell model.[3,15,29] It considers two different regions of water inside the nanopool. One region close to the AOT anionic head groups forming a shell of strongly bound water molecules and another one at the center or core of the RM where "free" water molecules whose behavior resembles that of bulk water. The latter is formed at W_0 sufficiently large that all of the AOT head groups are fully solvated, and it is nascent at a $W_0 \sim 5$.[30,31] We will use this model to discuss the observed change of the anisotropy parameters with the water content of RM.

To this end, at low W_0 values ($W_0 < 5$, regions I and II), the behavior of the short relaxation time (τ_R) increases equally for both forms (Figure 3), while the difference in S^2 does not show a significant change (Figure 5). On the contrary, the long relaxation times (τ_D) reach a maximum at $W_0 \sim 2$. Below this value, they are identical for both forms (region I, Figure 4A). Such behavior has been previously suggested to occur analyzing other parameters.[16,23] Calorimetric measurements for the average molar heat of water solution in AOT RM revealed a maximum at $\sim W_0 = 2$.[32] The result was explained in terms of a three-state model of water: two shells, one of them strongly attached to the AOT anionic head groups, and a water bulk-like core. Because the formation of the intermediate shell is an endothermic process and that of the bound shell one is exothermic, the curve shows a maximum at the water relative concentration where a likely bulk core starts to be formed. Nevertheless, the authors admitted that it was not possible to fit their model to the experimental data quantitatively and suggested that there could be another water aggregation state before the appearance of the bulk core at W_0 about 5. This three-layer state model is an improvement of the core−shell one explained already plus an intermediate layer of "polymeric" water in between the shell of strongly bound water and the bulk-like water core. Our results cannot definitively discern whether this or the core−shell model is more appropriate. They indicate that more effort should be done to consider the three-layer model in regards of the τ_D results. Moreover, such a similar three-layer model has also been invoked and applied for the hydration of proteins.[2] An equilibrium between the three layers was modeled and used to explain the dynamics of water around them.

Another work reported on a comparable behavior of the dielectric properties of AOT RM.[16] By means of terahertz time-domain spectroscopy, and using a two-component Debye model to fit the result, a strong size dependence of the low-frequency

mode amplitude was observed below $W_0 = 2-3$ and a smooth change in the high mode one up to $W_0 \sim 10$. The result was explained in terms of a strong reduction of the static dielectric constant of water in the RM. The origin of this effect was assigned to the suppression of a collective water relaxation mode because its correlation length is roughly 8 Å. The author suggested that the confinement effect has more influence on the nanopool behavior than the structural change of the H-bond network.[16]

Therefore, we looked for an explanation to our most interesting observation (Figure 4A). If one simply calculates the average density ($\langle \rho_{H_2O(POOL)} \rangle$) of water inside the RM using

$$\langle \rho_{H_2O(POOL)} \rangle = \frac{n_{H_2O(POOL)} M_{H_2O}}{N_A 4/3\pi \cdot r_{POOL}{}^3} \qquad (2)$$

where $n_{H_2O(POOL)}$ is the number of water molecules inside the RM,[33] M_{H_2O} is the water molar mass, N_A is Avogadro's number, and $r_{POOL}/\text{nm} = 1.5\ W_0$, then the change of the density shows a clear maximum at $W_0 = 1.5-2$ and a plateau for $W_0 = 5$ (Figure 4B). The behavior hence shows three different regions. It is remarkable that the two expected transitions using eq 2 are reminiscent to those of τ_D with W_0 (Figure 4A). This coincidence suggests that τ_D is related to the packing of water in the studied W_0 range. For $W_0 < 2$ (region I) as the packing (or density) increases, the lateral diffusion is more hindered, and vice versa at $2 < W_0 < 5$ (region II). Once the density has reached a plateau, in region III ($W_0 > 5$), there are enough water molecules to complete the shell of bound molecules solvating the AOT head groups, and therefore the added water molecules form the core. Note that it could be argued that the rising regime of the lateral diffusion time is connected to the rotational diffusion of the RM as a whole. This is rather unlikely because the rotational diffusion time of the RM is of about 25 ns at $W_0 = 0$, 10 times larger than the decay time observed here.[34]

Because we used [AOT] = 0.2 M and the surfactant aggregation numbers at $W_0 = 2$ and 5 are 26 and 42, respectively, the number of water molecules per micelle are $n_W = 52$ and 211.[33] Therefore, the number of water molecules per AOT head in region II changes from 2 to 5, approaching the full solvation of the AOT heads (consisting of six water molecules per headgroup)[30] as the values get to the plateau.

At W_0 values larger than 5, the variation of the three WIC fitting parameters show a plateau (Figures 3−5). A similar trend has been found, for example, when monitoring the stretching modes of the AOT sulfonate group:[30] a band shift was observed to change up to W_0 about 3−5, and almost not above 5. The results were explained in terms of the hydration of the head groups and the head-to-head interaction. As the solvation shell gets formed, the change in the IR spectrum is significant. Once the shell is formed, no more evolution in the bands is observed when increasing the RM water content. Our data reflect this behavior of the AOT nanopool (Figures 3−5). Another example is the study of the fluorescence characteristics of 8-anilino-1-naphtalene sulfonic acid (ANS), auramine-O, and the fluorescence quenching of Saphranine-T by inorganic ions as function of W_0.[31] In these cases, a sharp change in the trend of the observable (fluorescence maximum position, fluorescence intensity, quenching rate constant...) was recorded at about $W_0 = 5$ following the nanopool "microviscosity" obtained from the Auramine-O quantum yield fluorescence measurements.[31]

It is also noteworthy that the activity of water (a_W) inside the AOT RM reaches a plateau at similar values, with a value very similar to that of pure water, which is about 0.3 at low W_0.[3b] A correlation between the obtained τ_D values and the water activity is shown in the inset of Figure 4A, where the maximum of this parameter is found at $a_W \approx 0.7$.

The difference in the plateau heights of the order parameter (Figure 5) and the lateral relaxation time (Figure 4A) reveal either a different localization of both forms (E and K) as found for other compounds[35] or a change in the H-bond structure of the environment due to the proton-transfer process in bound E. For the latter, a variation in the apparent viscosity of the nanopool observing E or K fluorescence could be due to a reaction-induced fluidization of the water network inside the RM. This is due to the dynamics of the double proton-transfer reaction in E, leading to motion of surrounding water molecules. The apparent viscosities felt by E and K are about 30 cP and 10 cP, respectively, calculated by comparing the bulk water and the lateral diffusion time plateau values ($W_0 = 20$), taking into account that the rotational times are directly proportional to the viscosity. Thus, a structural change of water nanopool induced by the proton-transfer reactions leads to a change in the viscosity of water inside the RM. In none of the two structures of the probe, the long relaxation time (τ_D, Table 2) reaches the value of the rotational diffusion time of a molecule of this shape in pure bulk water (21 ps for a sphere of the same volume under stick boundary conditions, or about 35 ps for the longer component of an oblate rotating under stick boundary conditions). This suggests that either the 7HQ is never placed in the core of the RM or most probably that this core does not behave like bulk water. Furthermore, when a large amount of water molecules is trapped and bound next to the head groups of the AOT,[29] rotational diffusion of a probe inside the micelle might be affected by slow rotational time of confined water.

Recently, it was proposed that not all of the properties of water within the RM can be understood in terms of the core−shell model.[15a] Nonlinear time-resolved IR spectroscopy studies of AOT RM of W_0 from 2 to 60 have been used to test the model. [15a] Following the spectral and dynamical characteristics (IR absorption spectra, relaxation of the excited-state population, spectral diffusion, and orientational relaxation) of the O−D bond stretching mode of a 5% HOD-doped RM, the model was questioned and revised.[15a] It was mainly concluded that the so-called "static" observables (IR absorption spectra and relaxation of the excited-state population) can be explained within the frame of the core−shell model, whereas the "dynamical" (spectral diffusion and orientational relaxation) ones can not. The used argument relates the latter ones to the H-bond network dynamics of the nanopool. Even if two water zones or subensembles are well-defined separately, a shell of 0.4 nm thickness hydrating the AOT head groups from one side and a core of bulk-like water from the other side, the involved H-bond network couples both regions efficiently mixing their properties and thus leading to behaviors incompatible with the mentioned model. In fact, the core−shell water exchange process is supposed to proceed in a time scale longer than 10 ps,[15a] slow enough to have distinct spectral and population dynamics for each zone, but sufficiently fast to make any difference in orientational dynamics and in spectral diffusion between both zones disappear. It is noteworthy that the excess of vibrational energy in the nanopool can be transferred through the AOT head groups to the apolar phase within the same time scale.[17] Hence, because the relaxation times observed in our work are much longer than the water core−shell exchange time, this process cannot be observed in our measurements. Similarly, in femtosecond studies of the hydration layer dynamics of protein surfaces, the exchange time between free and bound water has

been found to proceed in a time scale of few tens of picoseconds.[2] This process involves the rotational and diffusional translation of water molecules, and the H-bond break and formation,[2] as in the case of RM.

As in protein studies, the confinement effect and the singular behavior of the interfacial water strongly affect the global observation. Moreover, we have found that the proton-transfer reaction in E to give K strongly affects the environment properties by decreasing its viscosity (fluidization) down to three times.

We will now consider and discuss the obtained data from the point of view of the diffusion coefficients of the two motion modes considered in the WIC model. Using the lateral diffusion relaxation time constant, the lateral translational diffusion coefficient can be calculated with[36]

$$D_{\mathrm{D}} = \frac{r_{\mathrm{POOL}}^2}{6\tau_{\mathrm{D}}} \tag{3}$$

where τ_{D} is the related time and r_{POOL} ($r_{\mathrm{POOL}}/\mathrm{nm} = 1.5\ W_0$) is the inner radius of the water nanopool, obtained using several experimental methods.[33] We have used directly the experimentally obtained radii in ref 33a interpolating when needed. Note that this relationship will lead to a quadratic increase of D_{D} with the pool radius even when the plateau of the experimental relaxation time was reached. This prediction thus contradicts the experimental observation. Another interpretation of this time considers it as related to the final unrestricted rotational motion, rather than to a lateral diffusion coefficient.[15a] In this case, D_{D} and τ_{D} are simply related by

$$D_{\mathrm{D}} = \frac{1}{6\tau_{\mathrm{D}}} \tag{4}$$

This relationship is much more senseful than eq 3 because once the shell is formed no significant change in the friction coefficient is expected. Furthermore, a plateau should be reached in the diffusion coefficient behavior at large W_0 values (see Figure 6B). At the W_0 corresponding to the maximum in τ_{D} (Figure 4A), a minimum is found for D_{D} (Figure 6B) but it is not as well-defined as the former.

The wobbling relaxation time τ_{R} relates to its diffusion coefficient D_{R} through the expression

$$D_{\mathrm{R}} = \frac{x_{\mathrm{R}}^2(1+x_{\mathrm{R}})^2\{\ln[(1+x_{\mathrm{R}})/2] + (1-x_{\mathrm{R}})/2\}}{\tau_{\mathrm{R}}(1-S^2)[2(x_{\mathrm{R}}-1)]} + \frac{(1-x_{\mathrm{R}})(6+8x_{\mathrm{R}}-x_{\mathrm{R}}^2-12x_{\mathrm{R}}^3-7x_{\mathrm{R}}^4)}{24\tau_{\mathrm{R}}(1-S^2)} \tag{5}$$

where $x_{\mathrm{R}} = \cos\theta$ and $S = {}^1/_2 \cos\theta(1+\cos\theta)$. In this case, we observed small changes for the corresponding diffusion coefficients at large W_0 values (see Figure 6A). Therefore, and in accordance with the previous studies in RM, monitoring the fluorescence anisotropy of the E and K forms of 7HQ leads to the following conclusion: above W_0 about 5, the RM nanopool dynamics does not change any longer because the solvation of the AOT head groups is completed at this value. When representing (not shown) the D_{R} and the D_{D} values as function of the inverse viscosity (taken from ref 13), the former shows an almost linear dependence for both forms of 7HQ, but not the latter. Again, this result indicates that in this case the confinement affects the behavior of D_{D} more than the medium viscosity.

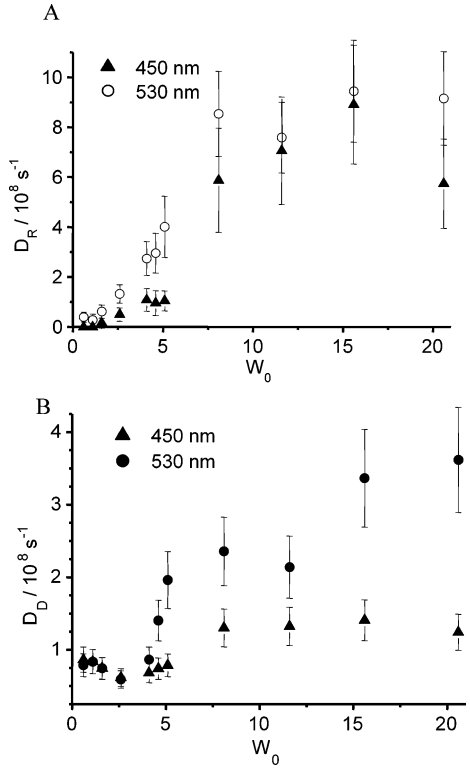

Figure 6. Effect of W_0 on (A) the diffusion coefficient for the wobbling relaxation (eq 5) and on (B) the longitudinal/final full orientational relaxation (eq 4). Full triangles, 450 nm; full circles, 530 nm.

4. Conclusions

We have shown that the anisotropy decay of a probe showing proton-transfer reactions 7HQ in the water nanopool confined inside AOT/*n*-heptane RM of increasing water content reveals different behaviors of the water-constrained network. Analyzed in terms of the wobbling-in-a-cone-model, the wobbling and lateral diffusion relaxation times, and the square of the order parameter, show a plateau above $W_0 \approx 5$. This value delimits a region below it where the bound water shell is still forming and above it where, although already formed, the dynamics is still much slower than that in pure bulk water. The difference in the plateau values of the square order parameter, and of the lateral diffusion relaxation time, for the bound E and the K forms is explained in terms of a more fluid environment felt by the latter but caused by double proton-transfer reactions in the former. A very interesting finding relates the bell-shaped lateral diffusion relaxation time dependence with W_0: it closely relates to the packing of water molecules in the nanopool. Following the change of τ_{D} with W_0, three regions have been identified: the first one ($W_0 = 0-2$) while forming the shell of bound water molecules to the AOT head groups for which the confinement effects dominate the relaxation dynamics; a second one ($W_0 = 2-5$) when increasing water content in the core region until it reaches the third region for which W_0 is larger than 5 and where no more significant change occurs.

Acknowledgment. This work was supported by the "Consejeria de Sanidad" of JCCM and MEC through projects SAN-04-000-00 and CTQ2005-00114.

References and Notes

(1) Robinson, G. W.; Zhu, S.-B.; Singh, S.; Evans, M. W. Eds. *Water in Biology Chemistry and Physics*; World Scientific: Singapore, 1996.
(2) Pal, S. K.; Zewail, A. H. *Chem. Rev.* **2004**, *104*, 2099.

(3) (a) Nandi, N.; Bhattacharyya, K.; Bagchi, B. *Chem. Rev.* **2000**, *100*, 2013. (b) Luisi, P. L.; Giomirfi, M.; Hleni, M. P.; Robinson, B. H. *Biochim. Biophys. Acta.* **1988**, *947*, 209.

(4) Chang, G.-G.; Huang, T.-M.; Hung, H.-C. *Proc. Natl. Sci. Counc. ROC(B)* **2000**, *24*, 89.

(5) Levinger, E. *Science* **2002**, *298*, 1722, and references therein.

(6) Cohen, B.; Huppert, D.; Solntsev, K. M.; Tsfadia, Y.; Nachliel, E.; Gutman, M. *J. Am. Chem. Soc.* **2002**, *124*, 7539.

(7) Klymchenko, A. S.; Demchenko, A. P. *Langmuir* **2002**, *18*, 5637.

(8) Kwon, O.-H.; Lee, Y.-S.; Yoo, B. K.; Jang, D.-J. *Angew. Chem., Int. Ed.* **2006**, *45*, 415.

(9) Hazra, P.; Chakrabarty, D.; Sarkar, N. *Langmuir* **2002**, *18*, 7872.

(10) Wittouck, N.; Negri, B. M.; Ameloot, M.; de Schryver, F. C. *J. Am. Chem. Soc.* **1994**, *116*, 10601.

(11) Kwon, O.-H.; Kim, T. G.; Lee, Y.-S.; Jang, D.-J. *J. Phys. Chem. B* **2006**, *110*, 11997.

(12) Hazra, P.; Chakrabarty, D.; Sarkar, N. *Chem. Phys. Lett.* **2003**, *371*, 553.

(13) Hasegawa, M.; Sugimura, T.; Shindo, Y.; Kitahara, A. *Colloids Surf., A* **1996**, *109*, 305.

(14) *Hydrogen-Transfer Reactions*; Hynes, J. T., Klinman, J. P., Limbach, H. H., Schowen, R. L., Eds.; Wiley-VCH: Weinheim, Germany, 2006; Vols. I and II.

(15) (a) Piletic, I. R.; Moilanen, D. E.; Spry, D. B.; Levinger, N. E.; Fayer, M. D. *J. Phys. Chem. A* **2006**, *110*, 4985. (b) Tan, H.-S.; Piletic, I. R.; Riter, R. E.; Levinger, N. E.; Fayer, M. D. *Phys. Rev. Lett.* **2005**, *94*, 057405. (c) Piletic, I. R.; Tan, H.-S.; Fayer, M. D. *J. Phys. Chem. B* **2005**, *109*, 21273. (d) Tan, H.-S., Piletic, I. R.; Fayer, M. D. *J. Chem. Phys.* **2005**, *122*, 174501.

(16) Mittelman, D. M.; Nuss, M. C.; Colvin, V. L. *Chem. Phys. Lett.* **1997**, *275*, 332.

(17) Deàk, J. C.; Pang, Y.; Sechler, T. D.; Wang, Z.; Dlott, D. D. *Science* **2004**, *306*, 473.

(18) (a) Sando, G. M.; Owrutsky, J. C. *J. Phys. Chem. B* **2006**, *110*, 9586. (b) Lee, Y. J.; Zhang, T.; Barbara, P. F. *J. Phys. Chem. B* **2004**, *108*, 5175. (c) Lee, Y. J.; Kee, T. W.; Zhang, T.; Barbara, P. F. *J. Phys. Chem. B* **2004**, *108*, 3474. (d) Gauduel, Y.; Pommeret, S.; Yamada, N.; Mingus, A.; Antonetti, A. *J. Am. Chem. Soc.* **1989**, *111*, 4974.

(19) Angulo, G.; Organero, J. A.; Carranza, M. A.; Douhal, A. *J. Phys. Chem. B* **2006**, *110*, 24231.

(20) (a) Mason, S. F.; Philp, J.; Smith, B. E. *J. Chem. Soc. A* **1968**, *12*, 3051. (b) Itoh, M.; Adachi, T.; Tokomura, K. *J. Am. Chem. Soc.* **1983**, *105*, 4828. (c) Park, H. J.; Kwon, O.-H.; Ah, C. S.; Jang, D.-J. *J. Phys. Chem. B* **2005**, *109*, 3938.

(21) Lipari, G.; Szabo, A. *Biophys. J.* **1980**, *30*, 489.

(22) Sen, S.; Sukul, D.; Dutta, P.; Bhattacharyya, K. *J. Phys. Chem. A* **2001**, *105*, 7495.

(23) Chakraborty, A.; Seth, D.; Setua, P.; Sarkar, N. *J. Phys. Chem. B* **2006**, *110*, 5359.

(24) (a)Zulauf, M.; Eicke, H.-F. *J. Phys. Chem.* **1979**, *83*, 480. (b) Riter, R. E.; Willard, D. M.; Levinger, N. E. *J. Phys. Chem. B* **1998**, *102*, 2705.

(25) Organero, J. A.; Tormo, L.; Douhal, A. *Chem. Phys. Lett.* **2002**, *363*, 409.

(26) Mateo, C. R.; Souto, A. A.; Amat-Guerri, F.; Acuña, A. U. *Biophys. J.* **1996**, *71*, 2177.

(27) Kinosita, K., Jr.; Kawato, S.; Ikegami, A. *Adv. Biophys*. **1984**, *17*, 147.

(28) Dutt, G. B. *J. Phys. Chem. B* **2004**, *108*, 7944.

(29) (a) Faeder, F.; Ladanyi, B. M. *J. Phys. Chem. B* **2001**, *105*, 11148. (b) Abel, S.; Sterpone, F.; Bandyopadhyay, S.; Marchi, M. *J. Phys. Chem. B* **2004**, *108*, 19458.

(30) Moran, P. D.; Bowmaker, G. A.; Cooney, R. P. *Langmuir* **1995**, *11*, 738.

(31) Glenn, K. M.; Palepu, R. M. *J. Photochem. Photobiol. A. Chem.* **2006**, *179*, 283.

(32) Goto, A.; Yoshioka, H.; Kishimoto, H.; Fujita, T. *Langmuir* **1992**, *8*, 441.

(33) (a) Wong, M.; Thomas, J. K.; Gratzel, M. *J. Am. Chem. Soc.* **1976**, *98*, 2391. (b) Chowdhury, P. K.; Ashby, K. D.; Datta A.; Petrich, J. W. *Photochem. Photobiol.* **2000**, *72*, 612. (c) Maitra, A. *J. Phys. Chem.* **1984**, *88*, 5122.

(34) Laia, C. A. T.; Costa, S. M. B. *Langmuir* **2002**, *18*, 1494.

(35) Aouida, M.; Rodgers, M. A. J. *J. Phys. Chem. B* **2003**, *107*, 6194.

(36) Maiti, N. C.; Krishna, M. M. G.; Britto, P. J.; Periasamy, N. *J. Phys. Chem. B* **1997**, *101*, 11051.